Time response parameters and control design for second-order nonminimum-phase systems

Marian J. BLACHUTA ⓘ , Robert BIEDA ⓘ and Rafał GRYGIEL ⓘ

The article considers the step and impulse response of second-order linear systems with a positive zero. A particular parameterization of the system equations is proposed which enables good assessment of the influence of its parameters on transients. Expressions missing in the literature are derived for step response parameters such as the values of undershoot, overshoot, time of inverse response, rise time and settling time, as well as of impulse response. Based on them, a precise time-domain approach to design feedforward, feedback and mixed feedback–feedforward control structures for nonminimum phase objects is presented that considers both setpoint tracking and disturbance rejection.

Key words: overshoot, undershoot, rise time, settling time, setpoint control, disturbance rejection, feedback–feedforward control

1. Introduction

Examples of second-order physical systems, usually nonlinear, with an inverse initial response can be found in the literature. For example, in [1] two process engineering plants can be found: an evaporator with variable heat transfer surface and a binary mixture separator. In [2] the Van de Vusse CSTR reactor is studied. The DC–DC boost converter [3, 4] is another example from the area of power electronics.

All authors are with Department of Automatic Control and Robotics, Silesian University of Technology, ul. Akademicka 2A, 44-100 Gliwice. M. Blachuta is the corresponding author (e-mail: Marian.Blachuta@polsl.pl).

Their linearized models can be expressed as transfer function $G(s)$ of the form

$$G(s) = \frac{a_0(1 - \tau s)}{s^2 + a_1 s + a_0}, \qquad a_0 > 0, \quad a_1 > 0, \quad \tau > 0 \tag{1}$$

with one positive zero $z_1 = 1/\tau$. The article is devoted to this particular model. An example of such model is used in [5] in the chapter summarizing the frequency-domain design of closed-loop control systems.

Nonminimum-phase systems, usually of higher order and with greater number of zeros, have been a subject of research for a long time, starting in the second half of previous century [6–8], and continuing until the present [9–15]. Most papers investigate nature of initial behavior of the step output. In particular [6] defines initial undershoot and states that undershoot occurs if and only if the plant has an odd number of real right-half plane zeros. A more detailed insight is given in [7], where conditions are examined under which there is no initial undershoot but the step output crosses the zero axis several times before finally going to a steady state. These results are valid for strictly proper transfer functions. Further discussion on the number of zero crossings and possible overshoot also for exactly proper transfer functions can be found in [11]. Further discussion of these concepts can be found in [12, 13]. Recently published article [15] extensively discusses initial and delayed undershoot and dependence of the step response on the initial condition.

Unfortunately, the literature lacks results regarding e.g. the values of under-shoot or overshoot, even for a simple system in (1). In contrast, the formulas derived in the article for this system precisely determine the values of all parameters characterizing the step response as shown in Fig. 1, and similar for the impulse response.
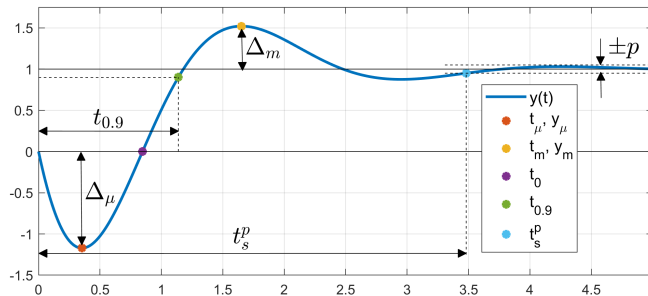
Figure 1: Step response of an nonminimum-phase oscillatory system and its characteristics: $\Delta_m = y(t_m) - 1$ – overshoot, $\Delta_\mu = -y(t_\mu)$ – undershoot, t_0 – zero crossing time, $(0, t_0)$ – interval of negative values of $y(t)$, $t_{0.9}$ – rise time to the level 0.9, i.e. $y(t_{0.9}) = 0.9$, t_s^p – settling time with tolerance p

Another group of problems concerns fundamental undershoot and settling time trade-offs in nonminimum-phase systems [9, 10] and trade-offs in feedback systems [8].

Although mathematically interesting, the qualitative results presented in [6–15] are rather irrelevant for the design of control.

Standard frequency domain methods developed for minimum-phase systems, based on concepts of phase and gain margin or sensitivity functions, are usually directly applied to nonminimum-phase ones [5, 16]. Unfortunately, except for ensuring stability, classical design specifications lead to poor control performance when applied to nonminimum-phase systems. It also is not possible to estimate the undershoot under this approach.

An attempt to adapt frequency domain methods to nonminimum-phase systems was presented in [17], where, in addition to classical concepts such as phase margin and crossover frequency, the controversial concept of a 'plateau' was introduced, which is to appear on the logarithmic plot of the modulus. Based on simulation studies, a number of nomograms combining step response parameters with parameters of frequency characteristics were created, constituting design tools. The method is limited to oscillatory setpoint tracking systems.

More direct methods base on the concept of plant-inversion feedforward that is directly applicable to minimum-phase plants. To extend this concept to nonminimum-phase plants, two alternative classes of feedforward design have been proposed in the literature: preview-based methods ([18] and references therein) and approximate-inverse methods [19–21]. Methods in the first class use preview information about the reference trajectory, while those in the second class attempt to approximate the unstable exact inverse of the plant model using a stable transfer function [22]. These ideas were also extended to nonlinear nonminimum-phase systems, see e.g. [23] and references therein. The feedforward path is usually a part of feedback–feedforward structure. However, there are no guidelines for designing the feedback loop that takes into account the response to disturbances. Another approach based on the theory of nonlinear control systems, summarized in [24] resulted in articles, e.g. [25, 26], was applied to nonlinear second-order nonminimum-phase chemical reactor systems. There are, however, no comparisons with other approaches. Reference [27] and references cited therein show large variety of solutions belonging to the so-called intelligent control methods such as fuzzy logic controllers, artificial neural networks, etc. often supported by soft computing tools.

This article focuses on a detailed discussion of the linear system in (1) and its control. Based on derived formulas for impulse and step responses and their parameters, a systematic approach to the precise design of both set-point tracking and disturbance rejection control systems for step change in set-point and

disturbance is presented. As a result, feedforward, feedback and mixed feedback–feedforward control structures are proposed taking into account the possible influence of noise and required control authority.

2. System model parameterization

In the control literature, the system in (1) is usually parameterized with the undamped frequency ω_n and damping factor ζ as follows

$$G(s) = \frac{\omega_n^2(1 - \tau s)}{s^2 + 2\zeta\omega_n s + \omega_n^2} = \frac{1 - \tau s}{T_n^2 s^2 + 2\zeta T_n s + 1} \,. \tag{2}$$

The article uses another parameterization based on poles, which better characterize transients. Depending on nature of the poles, the model in (1) can be written as follows

- for complex poles, $s_{1,2} = -\sigma(1 \pm j\theta) = -\sigma \pm j\omega$, with $\sigma = 1/T$ and $\omega = \sigma\theta = \theta/T$

$$G(s) = \frac{\sigma^2(1 + \theta^2)(1 - \tau s)}{s^2 + 2\sigma s + \sigma^2(1 + \theta^2)} = \frac{(1 + \theta^2)(1 - \tau s)}{T^2 s^2 + 2T s + (1 + \theta^2)} \,, \tag{3}$$

- for double pole $s_{1,2} = -\sigma$,

$$G(s) = \frac{\sigma^2(1 - \tau s)}{(s + \sigma)^2} = \frac{1 - \tau s}{(Ts + 1)^2} \,, \tag{4}$$

- and for different real poles, $s_1 = -\sigma$, $s_2 = -\sigma(1 + \phi)$

$$G(s) = \frac{\sigma^2(1 + \phi)(1 - \tau s)}{(s + \sigma)(s + \sigma(1 + \phi))} = \frac{(1 + \phi)(1 - \tau s)}{(Ts + 1)(Ts + 1 + \phi)} \,. \tag{5}$$

All these cases can be written in a common form

$$G(s) = \frac{a_0(1 - \tau s)}{s^2 + a_1 s + a_0} = \frac{b_0(1 - \tau s)}{T^2 s^2 + b_1 T s + b_0} \tag{6}$$

with

$$b_0 = \begin{cases} 1 + \theta^2, \\ 1, \\ 1 + \phi, \end{cases} \quad b_1 = \begin{cases} 2 & : \text{complex poles,} \\ 2 & : \text{double pole,} \\ 2 + \phi & : \text{different real poles} \end{cases} \tag{7}$$

and

$$a_0 = \sigma^2 b_0 = \frac{b_0}{T^2}, \qquad a_1 = \sigma b_1 = \frac{b_1}{T} \,. \tag{8}$$

The parameters $\sigma > 0$, $\theta > 0$ and $\phi > 0$ determine the position of the roots on the complex plane, as shown in Fig. 2b and T determines the time scale of transients. The coefficients b_0 and b_1 are dimensionless.
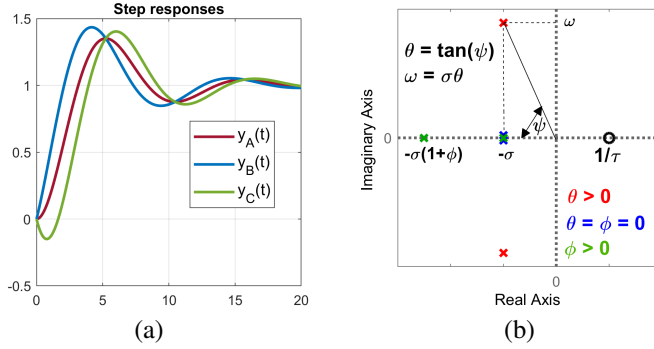
Figure 2: (a) The effect of zeros of systems in (9) on their step outputs. (b) Illustration of parameterization of transfer functions in (3)–(5). Note the intersections of all plots at the extrema of system A, half a period apart

.

The effect of zeros is shown in Fig. 2a where the time responses of three systems in (9) with $\sigma = 0.2$ $(T = 5)$, $\theta = 3$ are displayed.

$$G_A(s) = \frac{0.4}{s^2 + 0.4s + 0.4}, \qquad G_B(s) = \frac{0.4(1 + s)}{s^2 + 0.4s + 0.4}, \tag{9}$$

$$G_C(s) = \frac{0.4(1 - s)}{s^2 + 0.4s + 0.4}. \tag{10}$$

They all intersect in one point being the maximum of $y_A(t)$. As a result, regardless of the sign, each zero increases the overshoot.

The (σ, θ) parameters characterize oscillatory responses better than (ω_n, ζ). In particular, θ characterizes the decay of successive deviations from the steady state with the ratio $\Delta_{i+1}/\Delta_i = \mathrm{e}^{-\pi/\theta}$, where Δ_{i+1} is delayed with respect to Δ_i by π/ω, while σ determines the exponential decay of their envelopes. This directly implies the relationship between the overshoot Δ_m and undershoot Δ_μ:

$$\frac{\Delta_m}{\Delta_\mu + 1} = \mathrm{e}^{-\pi/\theta}. \tag{11}$$

For $\Delta_\mu = 0$ it becomes $\Delta_m = \mathrm{e}^{-\pi/\theta}$, i.e. the classical expression for the overshoot in a system with no zero. The formula in (11) is valid for any oscillatory transients and can be explicitly checked on equations in (31)–(32).

The relationships between the parameterizations (σ, θ) and (ζ, ω_n) are determined as

$$\sigma = \zeta \omega_n, \qquad\qquad \theta = \frac{\sqrt{1 - \zeta^2}}{\zeta}, \qquad (12)$$

$$\omega_n = \sigma \sqrt{1 + \theta^2}, \qquad\qquad \zeta = \frac{1}{\sqrt{1 + \theta^2}}. \qquad (13)$$

3. Time responses

The main goal is to find the analytical expressions for step response parameters as shown in Fig. 1. These parameters are: time t_μ and the value of maximum undershoot Δ_μ, zero crossing time t_0, time $t_{0.9}$ to reach 90% of the steady state, time t_1 to reach 1.0 for the first time, time of maximum overshoot t_m and maximum overshoot Δ_m, and the settling time t_s^p after which $y(t)$ reaches a value between $1 - p, 1 + p$. They are presented in Fig. 1.

In the control literature, e.g. [28], simple expressions are given to describe most of the parameters in the case of oscillatory systems, which, parameterized using (T, θ), take the simple form:

$$t_m = \frac{\pi}{\theta} T, \qquad \Delta_m = \mathrm{e}^{-\pi/\theta}, \qquad t_s^{0.02} \approx 4T. \qquad (14)$$

It should be noted, however, that although they are widely used, they are only valid for second-order systems without finite zero. Both negative and positive zeros invalidate these results, as can be seen from Fig. 2a for three systems with the same denominator and different numerators.

The famous inequality

$$\Delta_\mu \geqslant \frac{\beta}{\mathrm{e}^{z_1 t_\beta} - 1}. \qquad (15)$$

derived in [7] and repeated in [9, 10, 15] provides the lower bound on undershoot Δ_μ depicted in Fig. 1 for system with one positive zero z_1 as a function of z_1 and the rise time t_β to the level β.

This inequality expresses the fundamental limitation: that shortening the rise time to zero increases the undershoot to infinity. Unfortunately, (15) is the relation between two unknowns Δ_μ and t_β and reduces information about $G(s)$ to z_1. This makes (15) unlikely to be useful for estimation of Δ_μ. Indeed, the lower bound given by this result is quite conservative, particularly when the settling time is considered as in [9, 10], i.e. $t_\beta = t_s$ and $\beta = 1 - p \approx 1$.

Here and in further considerations a relative value λ of time constant τ, i.e.

$$\lambda = \frac{\tau}{T}, \qquad (16)$$

will be used.

The lower bound on the undershoot based on the inequality in (15) can be determined using numerically computed values of t_β. Fig. 3 shows that the lower limits are very conservative and as such is practically usesless.
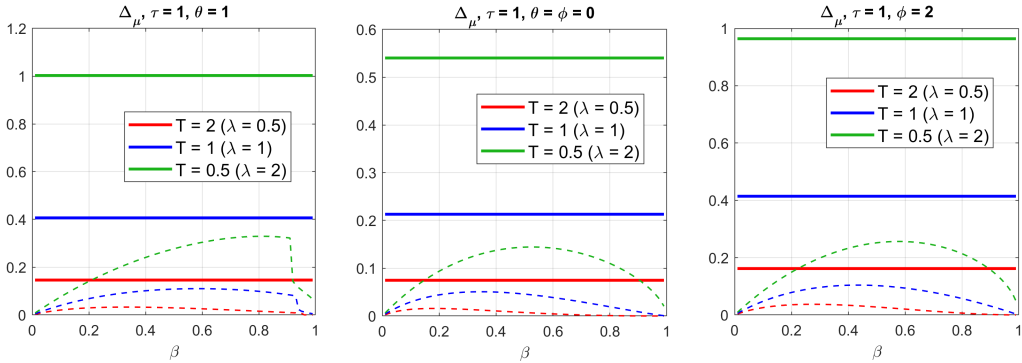
Figure 3: Comparison of the true values of undershoot in systems of Fig. 8 with their lower bounds resulting from the formula in (15). Solid lines – true values of Δ_μ, dashed lines – lower bounds of Δ_μ as functions of β

Therefore, the correct values of the step response parameters are found taking into account the actual system. This is the topic of the next section where exact analytic solutions are given for both step and impulse responses for complex, double and different real roots. The extrema of these functions were also found analytically, giving the values of undershoot and overshoot as well as the instants of their appearance.

3.1. Impulse response

Since the impulse response $g(t)$ is the first derivative of the step response $y(t)$, a time t_μ such that $g(t_\mu) = 0$ determines the undershoot of $y(t)$. Similarly, a time t_i such that $g(t)$ attains maximum determines the inflection point of $y(t)$.

Impulse response parameters are also important in disturbance rejection control design.

3.1.1. Analytic expressions for impulse responses

Depending on nature of roots there is

- for complex roots, $\theta > 0$

$$g(t) = \frac{\lambda(1 + \theta^2)\mathrm{e}^{-t/T}}{T \sin \varepsilon} \sin(\omega t - \varepsilon),$$

$$\varepsilon = \arctan \frac{\lambda\theta}{\lambda + 1}, \qquad \omega = \frac{\theta}{T},$$

(17)

- for double root, $\theta = \phi = 0$

$$g(t) = \frac{e^{-t/T}}{T} \left((\lambda + 1)t/T - \lambda\right), \tag{18}$$

- for real roots, $\phi > 0$

$$g(t) = \frac{(\lambda + 1)(1 + \phi)e^{-t/T}}{T\phi} \left(1 - \frac{(\lambda + 1 + \lambda\phi)e^{-\phi t/T}}{(\lambda + 1)}\right). \tag{19}$$

3.1.2. Examples of impulse responses

Examples of impulse responses are presented in Fig. 4–5 for the same parameters as step responses in Fig. 7–8.
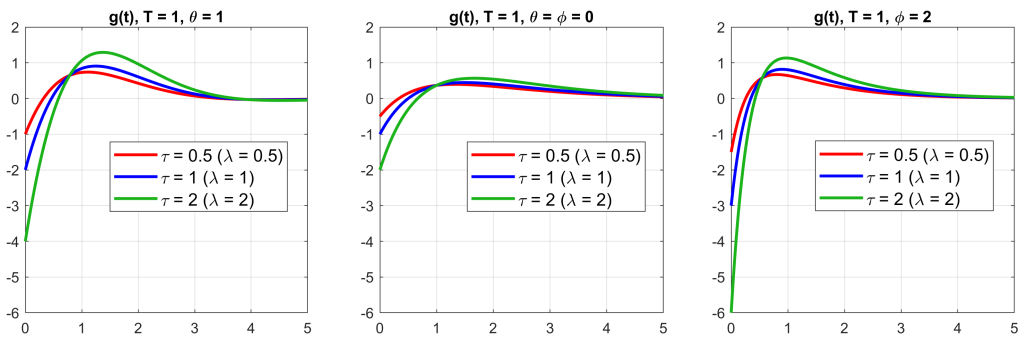
Figure 4: Impulse responses for systems with constant $T = 1$ and variable τ
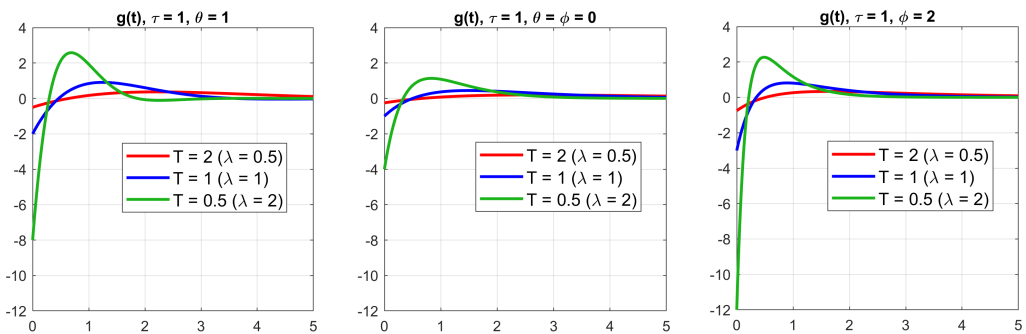
Figure 5: Impulse responses for systems with constant $\tau = 1$ and variable T

3.1.3. Parameters of impulse responses

The parameters $g(0^+)$, time t_μ and the maximum value of impulse responses can be expressed as follows

- for complex roots, $\theta > 0$

$$g(0^+) = \frac{-\lambda(1 + \theta^2)}{T}, \qquad t_\mu = \frac{T}{\theta} \arctan \frac{\lambda\theta}{\lambda + 1} = \frac{T\varepsilon}{\theta}, \qquad (20)$$

$$g_m = \frac{\lambda\theta\sqrt{1 + \theta^2}}{T \sin\varepsilon} e^{-t_i/T}, \qquad t_i = \frac{T}{\theta}(\arctan\theta + \varepsilon), \qquad (21)$$

- for double root, $\theta = \phi = 0$

$$g(0^+) = \frac{-\lambda}{T}, \qquad t_\mu = \frac{\lambda}{\lambda + 1}T, \qquad (22)$$

$$g_m = \frac{(\lambda + 1)}{T} e^{-t_i/T}, \qquad t_i = \frac{2\lambda + 1}{\lambda + 1}T, \qquad (23)$$

- for real roots, $\phi > 0$

$$g(0^+) = \frac{-\lambda(1 + \phi)}{T}, \qquad t_\mu = \frac{T}{\phi} \ln \frac{\lambda + 1 + \lambda\phi}{\lambda + 1}, \qquad (24)$$

$$g_m = \frac{1}{T} \left(\frac{(\lambda + 1)^{(1+\phi)}}{(1 + \phi)(\lambda + 1 + \lambda\phi)} \right)^{1/\phi}, \qquad (25)$$

$$t_i = \frac{T}{\phi} \ln \frac{(1 + \phi)(\lambda + 1 + \lambda\phi)}{\lambda + 1}. \qquad (26)$$
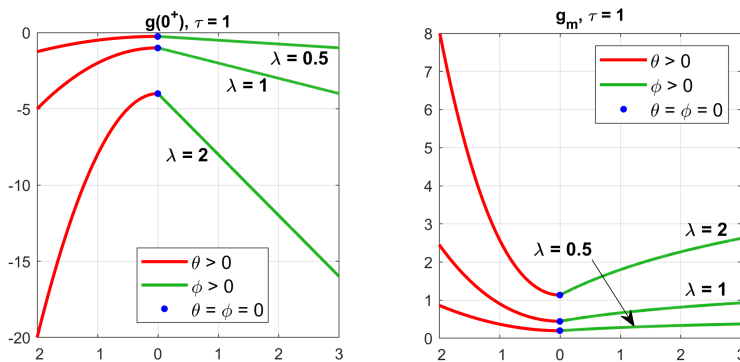
Figure 6: Impulse response parameters $g(0^+)$ and g_m for $\tau = 1$ and various T

3.2. Step response

3.2.1. Analytic expressions of step responses

Depending on nature of roots there is

- for complex roots, $\theta > 0$,

$$y(t) = 1 - \frac{e^{-t/T}}{\sin \varphi} \sin(\omega t + \varphi), \tag{27}$$

$$\varphi = \arctan \frac{\theta}{\lambda(1 + \theta^2) + 1}, \quad \omega = \frac{\theta}{T}, \quad \lambda = \frac{\tau}{T}, \tag{28}$$

- for double root, $\theta = \phi = 0$,

$$y(t) = 1 - e^{-t/T} \left(1 + (\lambda + 1)t/T \right), \tag{29}$$

- for real roots, $\phi > 0$,

$$y(t) = 1 - \frac{(\lambda + 1)(1 + \phi)e^{-t/T}}{\phi} \left(1 - \frac{(\lambda + 1 + \lambda\phi)e^{-\phi t/T}}{(\lambda + 1)(1 + \phi)} \right). \tag{30}$$

3.2.2. Examples

The influence of all parameters T, τ, θ or ϕ on the step output is presented on Fig. 7–8. Figure 7 is convenient for explaining the effect of change of zero with the denominator of the transfer function unchanged. Figure 8 shows the effect of changing the time scale T with the other parameters unchanged. This presentation is especially important for control systems where, for stability reasons, zero cannot be changed by the controller.

Looking at these graphs in a column way, it can be seen that for the same values of the ratio $\lambda = \tau/T$, although appearing at different times, the undershoot
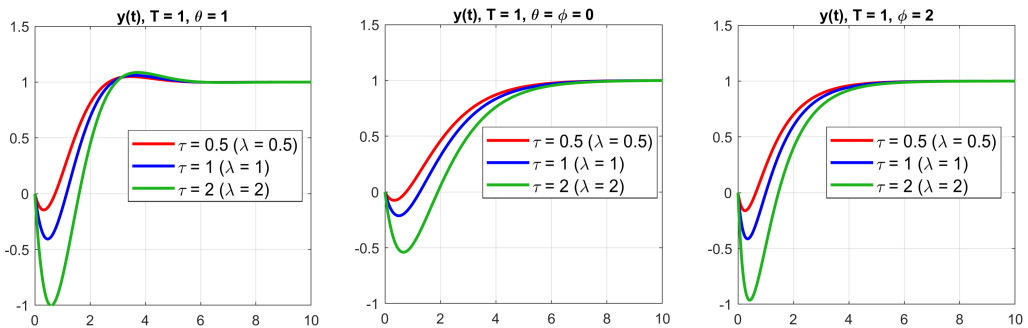
Figure 7: Step responses for systems with constant $T = 1$ and variable τ. For all of them, increasing τ increases the undershoot. Notice similarity of the responses of systems with $\theta = 1$ and $\phi = 2$ for $0 < t < t_0$
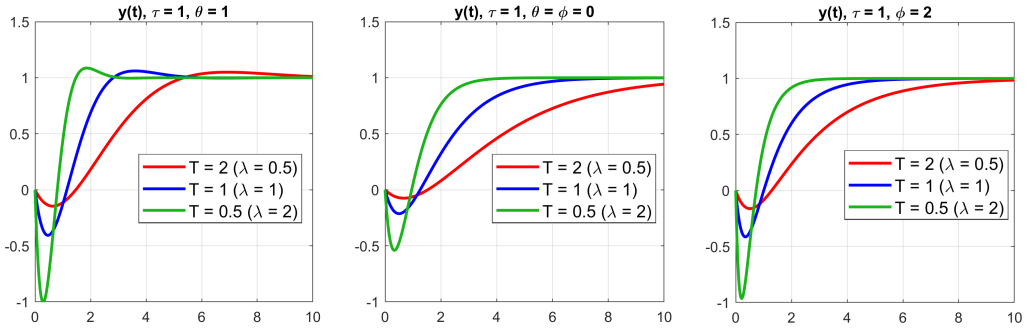
Figure 8: Step responses for systems with constant $\tau = 1$ and variable T. For all of them, decreasing T accelerates transients and increases the undershoot

values are the same. It is seen that increasing λ increases undershoot for all types of dynamics. It can also be seen, especially from the layout of the plots in the first row in Fig. 11, that the same λ shows similar undershooting behavior for certain pairs of oscillatory and non-oscillatory systems. However, then oscillatory systems reach 0.9 faster than the non-oscillatory ones, but at the cost of overshoot. The settling times for those systems are similar. It is also seen that the double pole system has the smallest undershoot at the cost of the slowest response.

3.2.3. Undershoot and overshoot

Based on expressions in (28)–(30) for step responses, the exact values are obtained of t_μ and t_m providing the minimum $y_\mu = y(t_\mu)$, the maximum $y_m = y(t_m)$ and t_1 such that $y(t_1) = 1$ for the first time.

- complex poles, $\theta > 0$,

$$y_\mu = -\Delta_\mu = 1 - \sqrt{(\lambda+1)^2 + (\lambda\theta)^2}\,\mathrm{e}^{-t_\mu/T},$$
$$t_\mu = \frac{T}{\theta}\arctan\frac{\lambda\theta}{\lambda+1}, \tag{31}$$
$$y_m = 1 + \Delta_m = 1 + \sqrt{(\lambda+1)^2 + (\lambda\theta)^2}\,\mathrm{e}^{-t_m/T},$$
$$t_m = \frac{T}{\theta}\left(\arctan\frac{\lambda\theta}{\lambda+1} + \pi\right), \tag{32}$$
$$t_1 = \frac{\pi - \varphi}{\theta}T. \tag{33}$$

- double pole, $\theta = \phi = 0$,

$$y_\mu = 1 - (\lambda+1)\mathrm{e}^{-t_\mu/T}, \quad t_\mu = \frac{\lambda}{\lambda+1}T, \tag{34}$$

• different real poles, $\phi > 0$,

$$y_\mu = 1 - \left(\frac{(\lambda + 1)^{(1+\phi)}}{\lambda + 1 + \lambda\phi} \right)^{1/\phi}, \quad t_\mu = \frac{T}{\phi} \ln \frac{\lambda + 1 + \lambda\phi}{\lambda + 1} . \quad (35)$$

Dependence of the undershoot Δ_μ and the overshoot Δ_m from λ for several values of θ and ϕ is presented in Fig. 9. It is worth noting that the variability of Δ_m and Δ_μ is much greater for oscillatory systems than for non-oscillatory ones. Other values such as t_0, $t_{0.9}$ and t_s can be found for the double pole case by using the Lambert $W(x)$ function [29, 30] exactly and only approximately in other cases. The results are summarized in the Appendix.
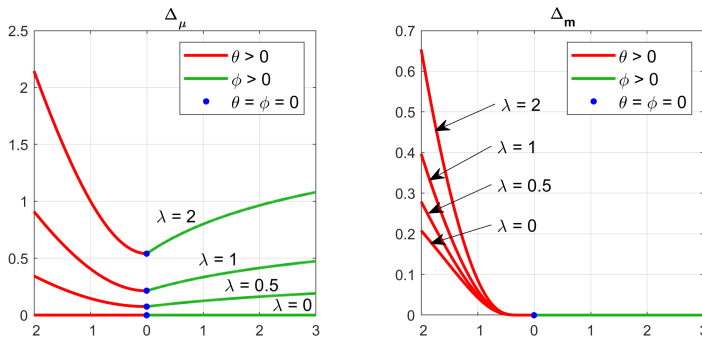
Figure 9: Undershoot Δ_μ and overshoot Δ_m as functions of θ and ϕ for different values of λ

To facilitate the use of formulas for characteristic values of impulse and step responses, MATLAB functions were developed. Their codes are listed in the Appendix.

4. Control

Two aspects of control can be distinguished: setpoint command control that provides reference following, and disturbance control aiming at suppressing the effect of disturbance. It is assumed here that $r(t) = 1(t)$ and $d(t) = 1(t)$ although in practical implementations rather certain smaller increments, e.g $r(t) = r_0 + \Delta r \cdot 1(t)$ and $d(t) = d_0 + \Delta d \cdot 1(t)$, come into play.

4.1. Setpoint command control

The obtained results can be used for the design of the set-point control entirely in the time domain. The problem statement consists of the plant $P(s)$

$$P(s) = \frac{\bar{y}(s)}{\bar{u}(s)} = \frac{a_0^p(1 - \tau s)}{s^2 + a_1^p s + a_0^p}, \quad (36)$$

the target transfer function of the controlled system $T(s)$

$$T(s) = \frac{\bar{y}(s)}{\bar{r}(s)} = \frac{a_0(1 - \tau s)}{s^2 + a_1 s + a_0} \tag{37}$$

and the sensitivity function $S(s) = 1 - T(s)$,

$$S(s) = \frac{s(s + a_1 + \tau a_0)}{s^2 + a_1 s + a_0}, \tag{38}$$

where $\bar{u}(s)$, $\bar{y}(s)$, $\bar{r}(s)$ are the Laplace transforms of $u(t)$, $y(t)$, $r(t)$, respectively. Note that $T(s)$ has the same zero as $P(s)$. Otherwise, the control system would be unstable.

The aim is to find a control structure along with an appropriate controller applied to $P(s)$ such that the target transfer function $T(s)$ is obtained. This can be done using either feedforward or feedback control structure, see Fig. 10a–b. Given plant $P(s)$ and desired dynamics $T(s)$, then a serial controller $Q(s)$, can be chosen such that

$$Q(s) = \frac{T(s)}{P(s)} = \frac{a_0}{a_0^p} \frac{s^2 + a_1^p s + a_0^p}{s^2 + a_1 s + a_0}. \tag{39}$$

The equivalent system can be obtained in the closed-loop structure with the controller

$$C(s) = \frac{Q(s)}{S(s)} = \frac{a_0}{a_0^p} \frac{s^2 + a_1^p s + a_0^p}{s(s + a_1 + \tau a_0)}, \tag{40}$$
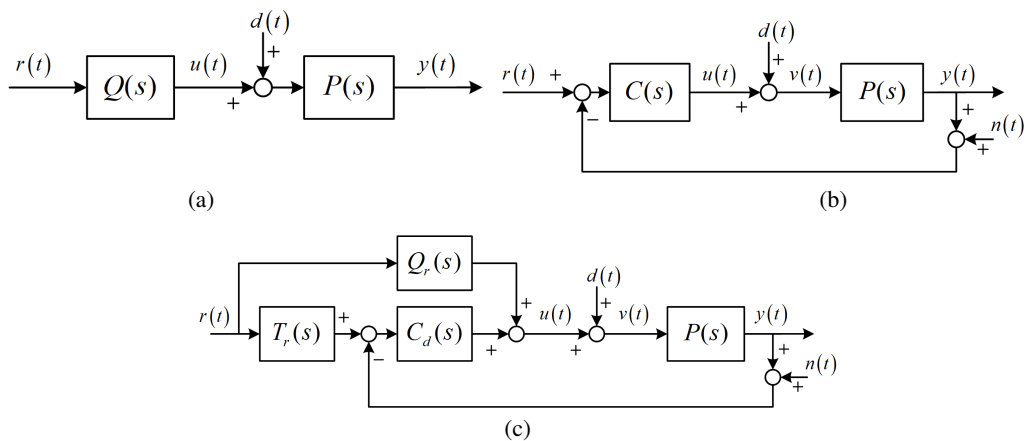
Figure 10: Control structures: (a) feedforward, (b) feedback and (c) feedback and feedforward. Signals: $r(t)$ – reference, setpoint; $u(t)$ – control signal; $y(t)$ – output, process variable; $d(t)$ – disturbance; $n(t)$ – measurement noise

which can be interpreted as a PID controller with an additional filter. From this
it follows that the initial value u_0 of the control signal is

$$u_0 = u(0^+) = \frac{a_0}{a_0^p} = \lim_{s \to \infty} Q(s), \tag{41}$$

which can limit the target dynamics given the limits of the control signal.

4.1.1. Design examples

Assume the plant $P(s)$

$$P(s) = \frac{0.4(1 - s)}{s^2 + 0.4s + 0.4}, \quad \text{with } T_p = 5, \ \theta_p = 3, \tag{42}$$

whose step response is depicted in Fig. 2 as $y_C(t)$, and target functions $T(s)$,
whose step responses and parameters are depicted in Fig. 8. Examples of repre-
sentative responses showing the influence of parameters λ, θ or ϕ are presented in
Fig. 11. Exemplary serial compensator for $T(s)$ with $\lambda = 1$, $T = 1$ and $\theta = \phi = 0$
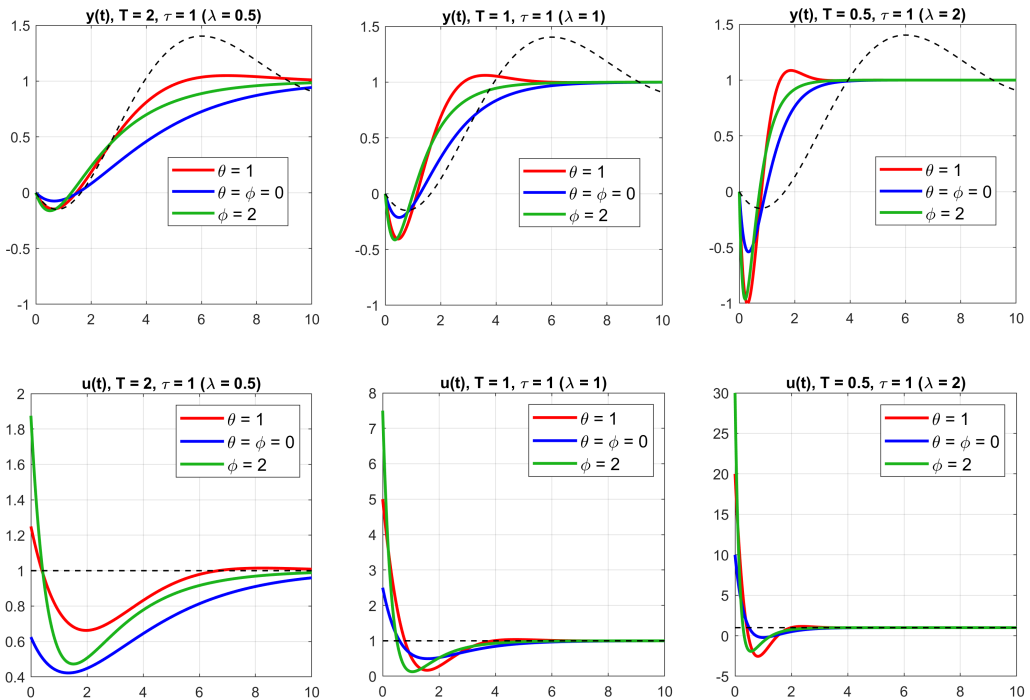
Figure 11: Step responses of control systems for the plant $P(s)$, whose dynamics are plotted with
a black dashed line and target dynamics as shown in Fig. 8

from Fig. 10a has the form

$$Q(s) = 2.5 \frac{s^2 + 0.4s + 0.4}{(s+1)^2} = \frac{2.5s^2 + s + 1}{(s+1)^2},$$ (43)

and the controller $C(s)$ for the closed-loop system in Fig. 10b

$$C(s) = 2.5 \frac{s^2 + 0.4s + 0.4}{s(s+3)} = 0.333 \frac{2.5s^2 + s + 1}{s(0.333s + 1)}.$$ (44)

Comparison of control signals shows that decreasing T from $T_p = 5$ to $T = 1$ results in increasing the value of u_0. For example the smallest value of $u(0^+)$ is for double root. For the controller in (44) it is

$$u_0 = \left(\frac{T_p}{T}\right)^2 \frac{1}{1 + \theta_p^2} = 5^2 \frac{1}{10} = 2.5.$$ (45)

Accelerating the transients by choosing $T = 0.5$ results in multiplying the values of u_0 by 4.

4.2. Disturbance rejection control

4.2.1. Simple feedback control

For the disturbance suppression the following transfer functions are important

$$\frac{\bar{u}_d(s)}{\bar{d}(s)} = -T_d(s) = -\frac{a_0(1 - \tau s)}{s^2 + a_1 s + a_0},$$ (46)

$$\frac{\bar{y}_d(s)}{\bar{d}(s)} = P(s)S_d(s) = \frac{s(s + a_1 + a_0\tau)(1 - \tau s)}{(s^2 + a_1 s + a_0)(s^2 + a_1^p s + a_0^p)}.$$ (47)

Observe also that

$$\frac{\bar{u}_d(s)}{\bar{d}(s)} = -\frac{\bar{y}_d(s)}{\bar{r}(s)}.$$ (48)

Disturbance responses $y_d(t)$ to $d(t) = 1$ displayed in Fig. 12 show that with decreasing T of the reference model $T(s)$, the magnitudes of responses $y_d(t)$ slowly decrease and their dependence on the type of dynamics slowly disappears. The dynamics of $y_d(t)$ remains, however, as sluggish as the dynamics of $P(s)$. The control signals $u_d(t)$ become faster. Observe that after a short time t_s, the control signal $u_d(t)$ reaches -1, and then $v(t) = 0$. As a result, the control system becomes open and the plant output $y_d(t)$ evolves as a free system with initial conditions obtained during the transition period of $v(t)$. An interesting peculiarity is that while for $t > t_s$ the controller's input $-y_d(t)$ varies in time, its

output $u(t)$ does not. This is explained by the fact that the series connection of $P(s)$ and $C(s)$ creates an unobservable system [31] in which zeros of $C(s)$ block the transients of the internal free variable $y_d(t)$ related to the same poles of $P(s)$.
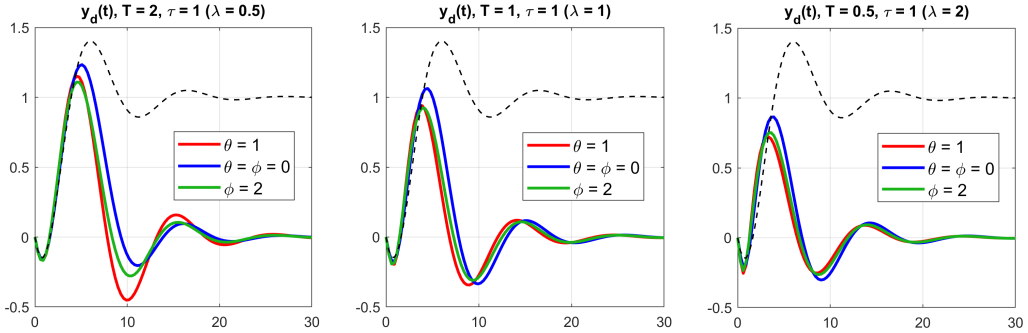
Figure 12: Disturbance responses in systems from Fig. 11

The behavior of the disturbance dynamics is easy to explain when the target dynamics becomes much faster than that of the plant. Then the signal $v(t) = u_d(t) + 1(t)$ controlling the plant can be approximated by the Dirac delta function, $v(t) = A\delta(t)$, with the area A

$$A = \int_0^\infty v(t)\,dt = \lim_{s \to 0} s \frac{1}{s}\left(\bar{u}_d(s) + \frac{1}{s}\right) \tag{49}$$

$$= \lim_{s \to 0}\left(\frac{1}{s} - \frac{a_0(1 - \tau s)}{s^2 + a_1 s + a_0}\frac{1}{s}\right) = \frac{a_1}{a_0} + \tau. \tag{50}$$

The same result can be obtained directly from the transfer function in (47) by replacing the fast dynamics represented by $(s + a_1 + a_0\tau)/(s^2 + a_1 s + a_0)$ with its steady-state gain $(a_1 + a_0\tau)/a_0$, which leads to

$$\frac{\bar{y}_d(s)}{\bar{d}(s)} \approx \left(\frac{a_1}{a_0} + \tau\right)\frac{s(1 - \tau s)}{s^2 + a_1^p s + a_0^p}. \tag{51}$$

Hence the step response $y_d(t)$ can be expressed by the impulse response $g_p(t)$ of the plant $P(s)$ as follows

$$y_d(t) \approx \left(\frac{a_1}{a_0} + \tau\right)g_p(t). \tag{52}$$

Assume, for example, the target $T(s)$ with $\theta = \phi = 0$, $\lambda = \tau/T$ and the oscillatory plant with θ_p and $\lambda_p = \tau/T_p$. Then, from (20), the maximum value y_m of $y_d(t)$

and t_m are determined by

$$y_m \approx \left(2\frac{T}{T_p} + \lambda_p\right) \frac{\lambda_p \theta_p \sqrt{1 + \theta_p^2}}{\sin \varepsilon} e^{-t_m/T_p}, \tag{53}$$

$$t_m = \frac{T_p}{\theta_p} (\arctan \theta_p + \varepsilon), \quad \varepsilon = \arctan \frac{\lambda_p \theta_p}{\lambda_p + 1}. \tag{54}$$

From (52) and (20)

$$y_\mu \approx y_d(0^+) = -\left(2\frac{T}{T_p} + \lambda_p\right) \lambda_p (1 + \theta_p^2), \tag{55}$$

where y_μ is the first minimum of $y_d(t)$.

The maximum value u_m of $u_d(t)$ results from formula (34) and equals to

$$u_m = (1 + \lambda)e^{-t_m/T} - 1, \quad t_m = \frac{\lambda}{\lambda + 1}T. \tag{56}$$

Note that since λ_p and θ_p are the plant parameters and $\lambda = \tau/T$, the only parameter that depends on the designer is T.

The accuracy of the approximations of y_m is very high. For example, for $\lambda = 2$ there is $y_m = Ag_m = 0.72$ for $\theta = 1$, $y_m = 0.87$, $Ag_m = 0.95$ for $\theta = \phi = 0$ and $y_m = 0.75$, $Ag_m = 0.79$ for $\phi = 2$. It can be seen that the accuracy for $\theta > 0$ and $\phi > 0$ is better than for $\theta = \phi = 0$. This is explained by graphs of $u_d(t)$ in Fig. 13 showing that the control signal for $\theta = \phi = 0$ is the slowest.

4.2.2. Mixed feedback–feedforward control

Speeding up the control system by making λ large would lead to large control signal when changing the setpoint. To resolve this contradiction, a feedback and feedforward control system can be used as in Fig. 10c, where $T_r(s)$ is obtained by feedforward and the faster $T_d(s)$ by feedback.

Exemplary controller for $\lambda = 4$, $T_d = 0.25$ and $\theta = \phi = 0$ has the form:

$$C_d(s) = 40\frac{s^2 + 0.4s + 0.4}{s(s + 24)} = 0.667\frac{2.5s^2 + s + 1}{s(0.042s + 1)}. \tag{57}$$

The high frequency gain 40 of this controller is 16 times greater than in (44). This means that the direct setpoint command following in a single loop system of Fig. 10b would require $u(0^+) = 40$ instead of 2.5 as in (43)–(44).

In the mixed feedback–feedforward structure, an appropriate compensator $Q_r(s)$ can be selected to arbitrarily limit the demand for large control signal values. However, if the increments Δr and Δd are small, the need for large control values can be reduced.
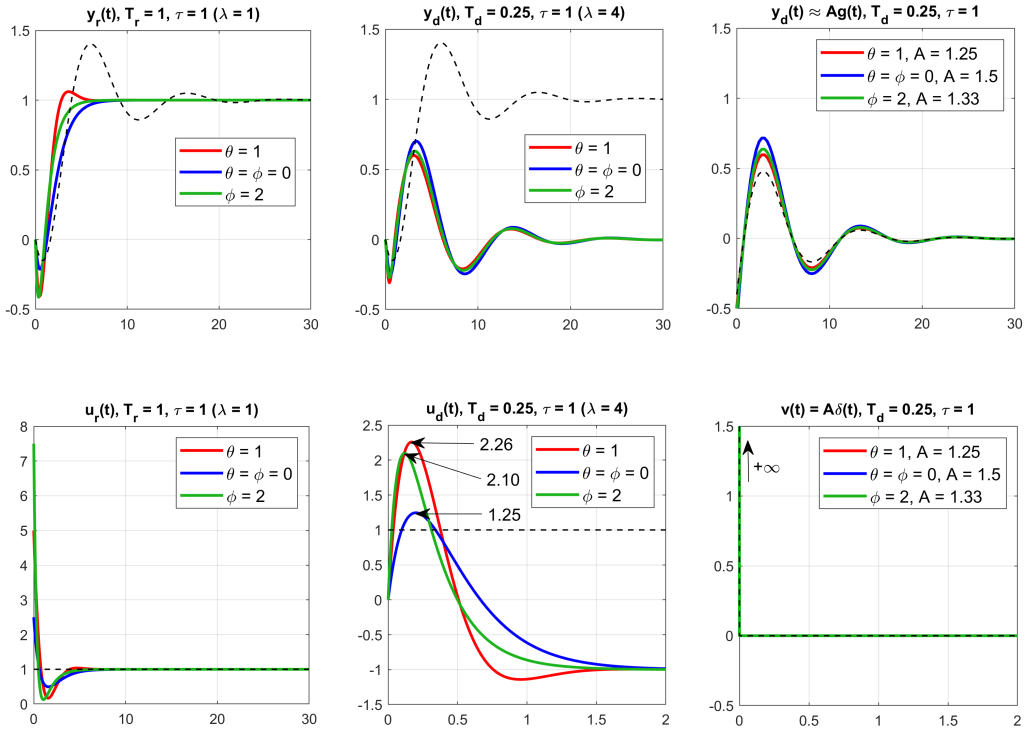
Figure 13: Signals in feedback–feedforward system in Fig. 10c. First column – setpoint command response, second column – disturbance response, third column – approximation of the disturbance response when the actual plant input signal $v(t) = u_d(t) + 1$ is replaced by $v(t) = A\delta(t)$. Dotted lines in the first two columns – step responses of the plant. Dotted lines in the third column show the limiting disturbance response for $\lambda \to \infty$. However, as explained further, the gain margin $\Delta L \to 1$, and the system tends to the border of stability

It should be noted that although the article focuses on the responses to step excitations, there are no obstacles to extending the analysis to include stochastic references, disturbances and noise in order to select controller parameters determining performance of output and control signals in terms of their variances or standard deviations.

4.3.   Gain margin

The gain margin ΔL, known from the Nyquist plot of $L(j\omega) = C(j\omega)P(j\omega)$ in classical frequency domain approach, determines the values of k for which the control system with the plant $kP(s)$, designed for the nominal value of $k = 1$, remains stable. It can also be found using the characteristic polynomial $\chi(s)$ of the closed loop system.

$$\chi(s) = k \, \text{num}\{C(s)\}\text{num}\{P(s)\} + \text{den}\{C(s)\}\text{den}\{P(s)\} \tag{58}$$

$$= a_0^p(s^2 + a_1^p s + a_0^p)\left(s^2 + (a_1 + a_0\tau(1 - k))\, s + ka_0\right). \tag{59}$$

For stability both polynomials in (59) should have positive coefficients, from which it follows

$$0 < k < \frac{a_1}{a_0\tau} + 1. \tag{60}$$

As a result

$$\Delta L = \frac{a_1}{a_0\tau} + 1 = \frac{b_1}{b_0}\lambda^{-1} + 1 = \frac{A}{\tau}, \tag{61}$$

where A is the area of the Dirac impulse in (50). Observe that since $a_1/(a_0\tau) = b_1/(b_0\lambda)$ is inversely proportional to λ, $\lim_{\lambda\to\infty} \Delta L = 1$, i.e. the system tends to the stability border. From (59), it oscillates then with the frequency

$$\omega = \frac{1}{T}\sqrt{b_1\lambda^{-1} + b_0}. \tag{62}$$

Gain margin can be considered as measure of robustness to plant gain changes.

5. Conclusions

The article presents the control design of second-order nonminimum-phase systems directly in the time domain, providing detailed information about the transients. Certain parameters of the step response, such as undershoot Δ_μ, overshoot Δ_m, and the times of their occurrence, are accurately determined regardless of the type of poles. Similar results were obtained for the impulse response.

Approximations are given for other values characterizing the step response, such as zero crossing time t_0, rise time $t_{0.9}$ and settling time t_s. The resulting formulas are implemented in MATLAB functions, which provide all results for the specified system.

The presented results allow the design of feedforward, feedback and combined feedback–feedforward controllers for both reference tracking and disturbance rejection.

The proposed parameterization enables good assessment of the influence of its parameters on transients, and thus their conscious selection. Therefore, the choice of the type of poles and values of the two parameters: T and θ or ϕ of a target transfer function $T(s)$ enables consideration of various constraints and often contradictory specifications including undershoot, overshoot, characteristic times t_0, $t_{0.9}$ and t_s, maximum value of control signal $u(0^+)$, maximum deviation

y_m of the output caused by disturbance, gain margin ΔL, etc. Numerous examples presented in the article support the development of engineering intuition in this direction.

The results are based on the assumption of linearity, accurate cancellation of zeros and poles and accurate knowledge of the gain of the object. The question arises about the impact of discrepancies between the model and the object or presence of unmodeled fast dynamics of actuators and sensors. The answer to this question is beyond the scope of this article. However, it can be said that the system has a certain degree of robustness depending on $\lambda = \tau/T$, where the higher λ, the worse the robustness.

It should be noted that, assuming a stochastic reference, disturbance, and noise, the controller parameters in designs can be optimized for the variance of the resulting control and control error signals or by minimizing more complex stochastic performance criteria.

All this can be considered as the basis for building an interactive control design system.

A. Crossing times t_0, $t_{0.9}$, t_1, and settling time t_s

A.1. Approximate formulas

The formulas approximating the crossing times depend on the character of poles.

- Complex poles, $\theta > 0$.

  The time t_0 to return to positive values is found as the intersection of the tangent calculated at the inflection point t_i with the zero axis. The rise time $t_{0.9}$ is calculated from the linear approximation of the output between t_0 and t_1. Settling time t_s^p is approximated by the time it takes for the exponential envelope to enter into the strip $[1 - p, 1 + p]$.

$$t_0 \approx t_i + \frac{2\theta - (1 + \theta^2) \sin \varphi e^{t_i/T}}{\theta(1 + \theta^2)} T, \qquad t_1 = \frac{\pi - \varphi}{\theta} T, \tag{A1}$$

$$t_i = t_\mu + \frac{T}{\theta} \arctan \theta, \qquad\qquad t_\mu = \frac{T}{\theta} \arctan \frac{\lambda\theta}{\lambda + 1}, \tag{A2}$$

$$t_{0.9} \approx \frac{t_0 + 9t_1}{10}, \qquad\qquad t_s^p \approx -T \ln(\sin \varphi p) \tag{A3}$$

  with

$$\varphi = \arctan \frac{\theta}{\lambda(1 + \theta^2) + 1}. \tag{A4}$$

- Double pole, $\theta = \phi = 0$.

  All time instants of interest can be found using the Lambert $W_{-1}(z)$ function [29, 30] defined as an infinite expansion

  $$W_{-1}(z) = \ln \cfrac{-z}{-\ln \cfrac{-z}{-\ln \cfrac{-z}{\cdots}}} . \tag{A5}$$

  Then denoting

  $$x = - \left(e^{-(\lambda+1)^{-1}} / (\lambda + 1) \right) \tag{A6}$$

  there is

  $$t_\mu = \frac{\lambda}{\lambda + 1} T, \tag{A7}$$

  $$t_0 = - \left(W_{-1}(x) + (\lambda + 1)^{-1} \right) T, \tag{A8}$$

  $$t_{0.9} = - \left(W_{-1}(0.1x) + (\lambda + 1)^{-1} \right) T, \tag{A9}$$

  $$t_s^p = - \left(W_{-1}(px) + (\lambda + 1)^{-1} \right) T. \tag{A10}$$

- Different real poles, $\phi > 0$

  $$t_0 \approx t_i + \cfrac{2 + \phi - \left((\lambda + 1 + \lambda\phi) \left(\dfrac{1 + \phi}{\lambda + 1} \right)^{(1+\phi)} \right)^{\frac{1}{\phi}}}{1 + \phi} T, \tag{A11}$$

  $$t_i = t_\mu + \frac{T}{\phi} \ln(1 + \phi), \quad t_\mu = \frac{T}{\phi} \ln \frac{\lambda + 1 + \lambda\phi}{\lambda + 1}, \tag{A12}$$

  $$t_{0.9} \approx -T \ln \frac{\phi}{10(\lambda + 1)(1 + \phi)}, \tag{A13}$$

  $$t_s^p \approx -T \ln \frac{\phi p}{(\lambda + 1)(1 + \phi)} . \tag{A14}$$

The results are shown in Fig. A1, where approximations of t_0, $t_{0.9}$ and $t_s^{0.02}$ are presented for both complex and real poles. The exact values obtained for the double poles are shown as blue dots. The actual values of $t_{0.9}$ and $t_s^{0.02}$ for $\lambda = 1$ obtained by the simulation are plotted with black lines.
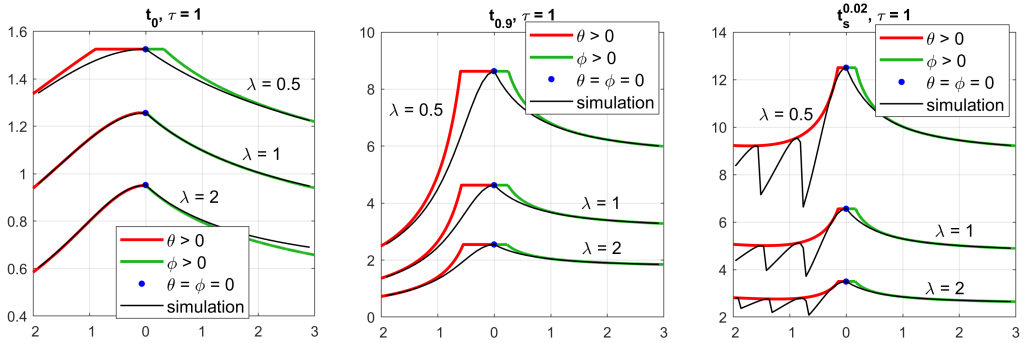
Figure A1: Times characterizing the step output: t_0 – time to return to positive values, $t_{0.9}$ – time to reach 0.9, $t_s^{0.02}$ – settling time with tolerance $p = 0.02$ as functions of θ or ϕ for various λ at constant τ. Since for $0 < \theta < 1$ and $0 < \phi < 1$ the approximations may deviate from the exact values they are bounded by values calculated for the double root case $\theta = \phi = 0$

A.2. MATLAB codes of NMP2IMPULSE and NMP2STEP functions

Function NMP2IMPULSE returns $g(0^+)$, g_m, and t_i. Function NMP2STEP returns Δ_μ, Δ_m, t_μ, t_m, t_0, $t_{0.9}$, t_1 and $t_s^{0.02}$ for given T, λ and θ or ϕ.

```matlab
function [g0,gm,ti] = nmp2impulse(varargin)
% ---Impulse Response Info for Second-Order Nonminimum-Phase Systems---
% [] = nmp2impulse(lambda,T,theta,'theta')  - Complex poles
% [] = nmp2impulse(lambda,T)  - Double pole
% [] = nmp2impulse(lambda,T,phi,'phi')  - Different real poles
%---------------------------------------------------------------%
n = length(varargin);
%
if n >= 2
  L = varargin{1};
  T = varargin{2};
  sys = 0;                  % Double pole
  if n == 4
  factor = lower(varargin{4});
  switch factor
    case 'theta'
      Th = varargin{3};
      if Th > 0, sys = 1; end % Complex poles
    case 'phi'
      Fi = varargin{3};
      if Fi > 0, sys = 2; end % Different real poles
  end
end
switch sys
  case 0
    g0 = -L/T;
    ti = (2*L+1)/(L+1)*T;
    gm = (L+1)*exp(-tm/T)/T;
  case 1
    g0 = -L*(1+Th^2)/T;
    psi = atan(L*Th/(L+1));
```

```matlab
      ti  = ( psi+atan(Th))/Th*T;
      gm = L*Th*(1+Th^2)^0.5*exp(-tm/T)/sin(psi)/T;
    case 2
      g0 = -L*(1+Fi)/T;
      ti  = log((1+Fi)*(L+1+L*Fi)/(L+1))/Fi*T;
      gm = (L+1)*((L+1)/(1+Fi)/(L+1+L*Fi))^(1/Fi)/T;
    end
  end
end % end nmp2impulse
```

MATLAB code for nmp2step function

```matlab
function [Du,Dm,tu,tm,t0,t90,t1,ts] = nmp2step(varargin)
% --Step Response Info for Second-Order Nonminimum-Phase Systems--
% [] = nmp2step(lambda,T,theta,'theta',{p}) - Complex poles
% [] = nmp2step(lambda,T,{p}) - Double pole
% [] = nmp2step(lambda,T,phi,'phi',{p}) - Different real poles
%--------------------------------------------------------------%
n = length(varargin);
%
if n >= 2
  L = varargin{1};
  T = varargin{2};
  sys = 0;                    % Double pole
  if n == 4 || n == 2, p = 0.02;   % p +- 2%
  else, p = varargin{end}; end
  if n >= 4
    factor = lower(varargin{4});
    switch factor
      case 'theta'
        Th = varargin{3};
        if Th > 0, sys = 1; end % Complex poles
      case 'phi'
        Fi = varargin{3};
        if Fi > 0, sys = 2; end % Different real poles
    end
  end
switch sys
  case 0
    tu = L/(L+1)*T;  Du = -(1-(L+1)*exp(-tu/T));
    tm = Inf;        Dm = 0;
      x = -exp(-1/(L+1))/(L+1);
      W = LambertW_Veberic(-1,x);
    t0  = -(W+1/(L+1))*T;
    t1  = Inf;
      W = LambertW_Veberic(-1,0.1*x);
    t90 = -(W+1/(L+1))*T;
      W = LambertW_Veberic(-1,p*x);
    ts  = -(W+1/(L+1))*T;
  case 1
    tu = atan(L*Th/(L+1))/Th*T;
    Du = -(1-((L+1)^2+(L*Th)^2)^0.5*exp(-tu/T));
    tm = tu +pi/Th*T;
    Dm = ((L+1)^2+(L*Th)^2)^0.5*exp(-tm/T);
      ti  = tu +atan(Th)/Th*T;
      psi = atan(Th/(1+L*(1+Th^2)));
    t0  = ti +(2*Th -(1+Th^2)*sin(psi)*exp(tp/T))/Th/(1+Th^2)*T;
```

```matlab
      t1  = ( pi−psi )/ Th∗T;
      t90 = ( t0 +9∗t1 )/10;
      ts  = −log ( sin ( psi )∗p)∗T;
    case 2
      tu  = log ((L+1+L∗Fi )/(L+1))/Fi∗T;
      Du  = −(1−(  (L+1)^(1+Fi )/(L+1+L∗Fi )  )^(1/Fi ));
      tm  = Inf ;         Dm = 0;
       ti = tu  +log (1+Fi )/Fi∗T;
      t0  = ti  +(2+Fi −((L+1+L∗Fi )∗((1+Fi )/(L+1))^(1+Fi ))^(1/Fi ))/(1+Fi )∗T;
      t1  = Inf ;
      t90 = −log ( Fi /(L+1)/(1+Fi )/10)∗T;
      ts  = −log (p∗Fi /(L+1)/(1+Fi ))∗T;
    end
    if  sys > 0
        x  = −exp (−1/(L+1))/(L+1); W = LambertW_Veberic(−1,x );
      t0_0  = −(W+1/(L+1))∗T;   W = LambertW_Veberic(−1,0.1∗x );
      t90_0 = −(W+1/(L+1))∗T;  W = LambertW_Veberic(−1,p∗x );
      ts_0  = −(W+1/(L+1))∗T;
      t0  = min ( t0 , t0_0 );
      t90 = min ( t90 , t90_0 );
      ts  = min ( ts , ts_0 );
    end
  end
end
end % end nmp2step

%%%%%%%%%%%%%%%%%%%%%%%%%%%%%%%%%%%%%%%%%%%%%%%%%%%%%%%%%%%%%%%%%
function  W = LambertW_Veberic( k , z )
% Darko  Veberic ,  "Having  Fun  with  Lambert  W( x )  Function"
% W_k( z ) = LambertW_Veberic ( k , z )
% k = 0  or  −1
%−−−−−−−−−−−−−−−−−−−−−−−−−−−−−−−−−−−−−−−−−−−−−−−−−−−−−%
it  = 1e3 ; % liczba  iteracji
e = exp (1);
%
if  k == 0
  if  z >= −1/e  && z < e
    W = z ;
     for  i  = 1: it , W = z / exp (W); end
  else
    W = log ( z );
     for  i  = 1: it , W = log ( z /W); end
  end
elseif  k == −1
  if  z >= −1/e  && z < 0
    W = log (−z );
     for  i  = 1: it , W = log (−z /(−W)); end
  elseif  z == 0, W = −Inf ;
  else , W = NaN;
  end
end
end % end LambertW_Veberic
```

References

[1] B. ROFFEL and B. BETLEM: *Process Dynamics and Control: Modeling for Control and Prediction*. John Wiley & Sons, 2006.

[2] J.G. VAN DE VUSSE: Plug-flow type reactor versus tank reactor. *Chemical Engineering Science*, **19**(12), (1964), 994–996. DOI: 10.1016/0009-2509(64)85109-5

[3] M. KAZIMIERCZUK: *Pulse-width Modulated DC–DC Power Converters*. John Wiley & Sons, 2016. DOI: 10.1002/9781119009597

[4] ZENGSHI CHEN, WENZHONG GAO, JIANGANG HU and XIAO YE: Closed-loop analysis and cascade control of a nonminimum phase boost converter. *IEEE Transactions on Power Electronics*, **26**(4), (2011), 1237–1252. DOI: 10.1109/TPEL.2010.2070808

[5] S. SKOGESTAD and I. POSTLETHWAITE: *Multivariable Feedback Control – Analysis and Design*. John Wiley & Sons, 2001.

[6] M. VIDYASAGAR: On undershoot and nonminimum phase zeros. *IEEE Transactions on Automatic Control*, **AC-31**(5), (1986), 440–440. DOI: 10.1109/TAC.1986.1104289

[7] B.A. LEÓN DE LA BARRA: On undershoot in SISO systems. *IEEE Transactions on Automatic Control*, **39**(3), (1994), 578–581. DOI: 10.1109/9.280763

[8] D.P. LOOZE and J.S. FREUDENBERG: Right half plane poles and zeros design tradeoffs in feedback systems: *IEEE Transactions on Automatic Control*, **AC-30**(6), (1985), 555–565. DOI: 10.1109/TAC.1985.1104004

[9] K. LAU, R.H. MIDDLETON and J.H. BRASLAVSKY: Undershoot and settling time tradeoffs for nonminimum phase systems. *IEEE Transactions on Automatic Control*, (**AC-48**)(8), (2003), 1389–1393. DOI: 10.1109/TAC.2003.815025

[10] J. STEWART and D.E. DAVISON: On overshoot and nonminimum phase zeros. *IEEE Transactions on Automatic Control*, **AC-51**(8), (2006), 1378–1382. DOI: 10.1109/TAC.2006.878745

[11] J.B. HOAGG and D.S. BERNSTEIN: Nonminimum-phase zeros – much to do about nothing. *IEEE Control Systems Magazine*, **27**(3), (2007), 45–57. DOI: 10.1109/MCS.2007.365003

[12] J.M. MACIEJOWSKI: Right-half plane zeros are not necessary for inverse response. *2018 European Control Conference (ECC)*, (2018), 2488–2492. DOI: 10.23919/ECC.2018.8550187

[13] S. ENGELBERG: Undershoot and overshoot: Testing the limits of rules of thumb. *IEEE Control Systems Magazine*, **38**(6), (2018), 87–91. DOI: 10.1109/MCS.2018.2851087

[14] T. DAMM and L.M. MUHIRWA: Zero crossing, overshoot and initial undershoot in the step and impulse responses of linear systems. *IEEE Transactions on Automatic Control*, **AC-59**(7), (2013), 1925–1929. DOI: 10.1109/TAC.2013.2294616

[15] M. KAMALDAR, S. ASEEM UL ISLAM, J. HOAGG and D. BERNSTEIN: Demystifying enigmatic undershoot in setpoint command following. *IEEE Control Systems Magazine*, **42**(1), (2022), 103–125. DOI: 10.1109/MCS.2021.3122270

[16] J.M. DIAZ, R. COSTA-CASTELLO and S. DORMIDO: Closed-loop shaping linear control systems design. *IEEE Control Systems Magazine*, **39**(5), (2019), 58–74. DOI: 10.1109/MCS.2019.2925255

[17] S. ENGELL, G. NÖTH, and J. PANGALOS: Indirect controller synthesis for systems with a zero in the right s-halfplane. (In German). *Regelungstechnik*, **30**(7), (1982), 232–239. DOI: 10.1524/auto.1982.30.112.232

[18] Q. Zou: Optimal preview-based stable-inversion for output tracking of nonminimum-phase control systems. *Automatica*, **45**(1), (2009), 230–237. DOI: 10.1016/j.automatica.2008.06.014

[19] J.A. Butterworth, L.Y. Pao *and* D.Y. Abramovitch: Analysis and comparison of three discrete-time feedforward model-inverse control techniques for nonminium-phase systems. *Mechatronics*, **22**(5), (2012), 577–587. DOI: 10.1016/j.mechatronics.2011.12.006

[20] B.P. Rigney, L.Y. Pao, and D.A. Lawrence: Nonminimum phase dynamic inversion for settle time appplication. *IEEE Transactions on Control Systems Technology*, **17**(5), (2009), 989–1005. 10.1109/TCST.2008.2002035
Nonminimum phase adaptive inverse control for settle performance applications. *Mechatronics*, **20**(1), (2010), 35–44. DOI: 10.1016/j.mechatronics.2009.06.007

[21] M.M. Michałek: Fixed-structure feedforward control law for minimum- and non-minimumum-phase LTI SISO systems. *IEEE Transactions on Control Systems Technology*, **24**(4), (2016), 1382–1393. DOI: 10.1109/TCST.2015.2487861

[22] M.R. Buchner and P.J. Young: Perfect tracking for nonminimum-phase systems. *2010 American Control Conference (ACC)*, (2010), 4010–4015. DOI: 10.1109/ACC.2010.5530431

[23] K.Graichen, V. Hagenmeyer and M. Zeits: Van de Vusse CSTR as a benchmark problem for nonlinear feedforward control design techniques. *2004 IFAC Nonlinear Control Systems*, (2004) 1123–1128. DOI: 10.1016/S1474-6670(17)31377-0

[24] A. Isidori: *Nonlinear Control Systems: An Introduction.* Springer, Berlin, Heidelberg, 1989. DOI: 10.1007/BFb0006368

[25] C. Kravaris and P. Dauoitidis: Nonlinear state feedback control of second-order nonminimum-phase nonlinear systems. *Computers & Chemical Engineering*, **14**(4-5), (1990), 439–449. DOI: 10.1016/0098-1354(90)87019-L

[26] C. Kravaris and P. Daoutidis: Output feedback control of nonminimum-phase non-linear processes. *Chemical & Engineering Science*. **49**(13), (1994), 2107–2122. DOI: 10.1016/0009-2509(94)E0009-F

[27] C.A. Márquez-Vera, M.A. Màrquez-Vera, Z. Yakoub, A. Ma'arif, A.J. Castro-Montoya and N.R. Cázarez-Castro: Fuzzy state feedback with double integrator and anti-windup for the Van de Vusse reaction, *Archives of Control Sciences*, **32**(2), (2022), 383–408. DOI: 10.24425/acs.2022.141717

[28] G.F. Franklin, J.D. Powell and A. Emami-Naeini: *Feedback Control of Dynamic Systems*, Prentice Hall, 2014.

[29] R.M. Corless, G.H. Gonnet, D.E.G. Hare, D.J. Jeffrey, and D.E. Knuth: On the Lambert W function. *Advances in Computational Mathematics*, **5** (1996), 329–359. DOI: 10.1007/BF02124750

[30] D. Veberic: Having fun with Lambert W(x) function. arXiv:1003.1628v1 [cs.MS], (2010). DOI: 10.48550/arXiv.1003.1628

[31] G.C. Goodwin, S.F. Graebe and M.E. Salgado: *Control System Design*. Prentice Hall, 2001.